2019 16th International Conference on Electrical Engineering, Computing Science and Automatic Control (CCE)
Mexico City, Mexico. September 11-13, 2019

Frequency-Swept Electronic Driver for Wideband Applications of Air-Coupled Ultrasound Transducers

Raul Daniel Casillas Mendoza
Instituto Nacional de Rehabilitación - Universidad La Salle, Subdirección de Investigación Biotecnológica, DIIM,
México City, México.
rdaniel.csmz@gmail.com

Josefina Gutiérrez Martínez
Instituto Nacional de Rehabilitación, División de Investigación en Ing. Médica,
México City, México.
jgutierrez@inr.gob.mx

Lorenzo Leija Salas
Department of Electrical Engineering/Bioelectronics CINVESTAV-IPN
México City, México.
lleija@cinvestav.mx

Arturo Vera Hernández
Department of Electrical Engineering/Bioelectronics CINVESTAV-IPN
México City, México.
arvera@cinvestav.mx

Mario Ibrahín Gutiérrez
CONACYT – Instituto Nacional de Rehabilitación, Subdirección de Investigación Biotecnológica, DIIM,
México City, México.
m.ibrahin.gutierrez@gmail.com

Abstract — **The ultrasound is a common way to measure the distance or detect an object. This is usually carried out by measuring the time-of-flight of the received echoes reflected by the objects, which is a parameter easily obtained from the signal and that only provides the spatial location. In the present paper, it is presented an electronic signal generator to drive air-coupled ultrasound transducers in a wideband regime. This design is planned to be used as a new application of these sensors, normally used for distance measuring, which is to characterize materials by using the complete signal of the echo to extract more useful information. The design was made with simple materials, but mainly based on a programmed microcontroller capable of making a specified frequency sweep that allows us to create a moderate-power tone burst with the use of a switched amplifier at the output. The tone burst produced by the microcontroller varies the pulse-width in time, obtaining the controllable frequency sweep that has a wide excitation spectrum.**

Keywords — **air coupled transducers, pulse generator, frequency sweep, object characterization**

I. Introduction

The use of the pulse-echo ultrasound (US) in obstacle detection systems has increased gradually. These systems are based on one or two air coupled ultrasound transducers and a processing system to send/receive the signal and postprocess it to get the distance information [1], [2]. These air coupled ultrasonic transducers are used, nowadays, for a lot of new applications like parking sensors in cars, and human-machine interfaces, e.g. touchless gesture recognition systems [3]. However, the more common reported devices use the ultrasound time-of-flight to determine the distance to the objects, which limits the total information that it could be extracted with ultrasound from the tested object [2]. Using only that parameter would be one of the more simplified ways for obstacle detection that ignores other possible parameters that could give more relevant data of the analyzed object [4]. To the best of our knowledge, analysis using the complete ultrasound wave of pulse-echo ultrasound in air for obstacle detection/characterization has not been widely reported.

The electronic devices for air coupled ultrasonic obstacle detection are usually simplified for easily determining the time-of-flight of the received signal [5]. Therefore, for this application, electronics is very simple and economically accessible for prototyping [6]. Extracting more information from the reflected wave requires different electronic designs to produce a short wideband ultrasound emission and to receive the reflected echoes [7]. These circuits should be designed based on the specific characteristics of the currently available air coupled wideband ultrasound transducers or based on our specially customized transducers [8], [9].

In this work, a wideband switched mode amplifier to drive a commercial air-coupled ultrasound transducer is presented. The system is composed by a wave generator, an emission amplifier and a reception system. Control of emission and parameter extraction (postprocessing) is carried out in a microcontroller.

II. Methodology

In this project, we are developing an air coupled ultrasound transceiver to determine the acoustic characteristics of materials. As a first approach, it is planned to drive inexpensive commercial transducers widely used in other applications; however, the use of customized transducers is not discarded in future works. The overall design is composed by a low power pulse generator, a switched amplifier, and the air-coupled ultrasound transducer for emission.

978-1-7281-4840-3/19/$31.00

The generator should provide a frequency controlled output capable of producing a chirp in the range of frequencies the transducer emits and receives efficiently [8]. In this work, we are using the air-coupled transducer B01JHOX3H6 (Cyanalab, China), which works efficiently in a band regime from 35 kHz to 45 kHz, centered at 40 kHz [4]. Therefore, for the purposes of this work, the generator should produce a short signal sweeping from 30 kHz to 50 kHz to fully cover the transducer wideband (obviously we are not using the extra regions in which the transducer is not reliable).

A. Low power pulse generator

This generator was made using a microcontroller. This device provides a square digital signal with a precisely controlled timing for the low and high state of each semi-cycle. The signal was programmed to be produced in a frequency range of 30 kHz to 50 kHz. This microcontroller will be used subsequently to process the received signal of the reception transducer [4].

The chosen microcontroller was the PIC16F887 with a 20 MHz crystal to be able to generate the pulses in the required times for each semi-cycle; each group of instructions for changing the output should last no more than 10 µs (half period of 50 kHz). Timing was determined offline and loaded in the data memory of the microcontroller to reduce time for calculations at each cycle. The program was made in assembly language. A trigger pulse was required for synchrony (see Fig. 1). This proposal was based on a microcontroller, but other techniques were analyzed (pulse width modulator, integrated signal generators, phase-locked loop, etc.) with limitations when controlling the required time variations at each half cycle; varying the time of each half cycle is not possible in such alternatives, since those require a stable frequency (period) for a larger time.

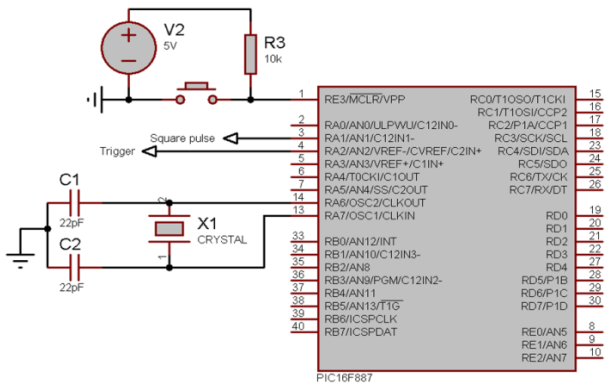

Fig. 1. Microcontroller circuit that produce the controlled-width pulse and the trigger.

B. Power amplifier

The medium power amplifier was based on a transistor working in switch mode. The theoretical efficiency of this configuration can be as large as 100%, under certain conditions. Because this design does not require high power, and the load (the transducer) is complex, the efficiency would not be smaller. The amplifier circuit in Fig. 2 shows a transistor being activated through an inverted buffer by the square pulse coming from the pulse generator. Inversion of the signal is required as the operation of the switch is inverted, because the output voltage at the transducer (TE) is positive when the transistor Q1 is switched off.

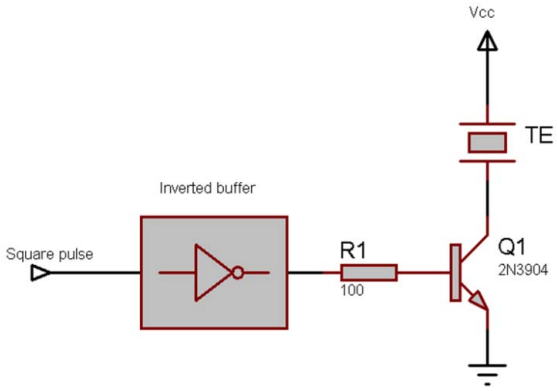

Fig. 2. Switched amplifier for ultrasound emission. The transducer (TE) is in series with the power transistor.

C. Reception circuit

The reception circuit was made with OPA27. The floating signal coming from the reception transducer was referenced to ground and amplified using a differential amplifier. Then, the signal was filtered using a low pass filter with cutoff frequency at 60 kHz. Signal postprocessing was made in MATLAB (MathWorks, USA).

III. Results and Discussion

A. Low power pulse generator

The pulse generator was programed in the microcontroller using assembly language. The calculation of the output times were made using the number of clock cycles required for each instruction of the code. However, differences in the programed/expected and measured times were obtained. In Fig. 3, measurements of the time of the first and last cycle at the output of the low power pulse generator are shown. The expected time values to get a half cycle of the initial and last frequencies, i.e. 30 kHz and 50 kHz, were 16.60 µs and 10.00 µs, respectively. Measured values were 15.50 µs and 9.49 µs, which gave a constant error of about 0.80 µs (SD: +0.02 µs) probably coming from a non-accounted instruction that lasted more than we expected. However, those values were enough to obtain a frequency sweep from 32.2 kHz to 52.7 kHz that is useful for the purposes of the system.

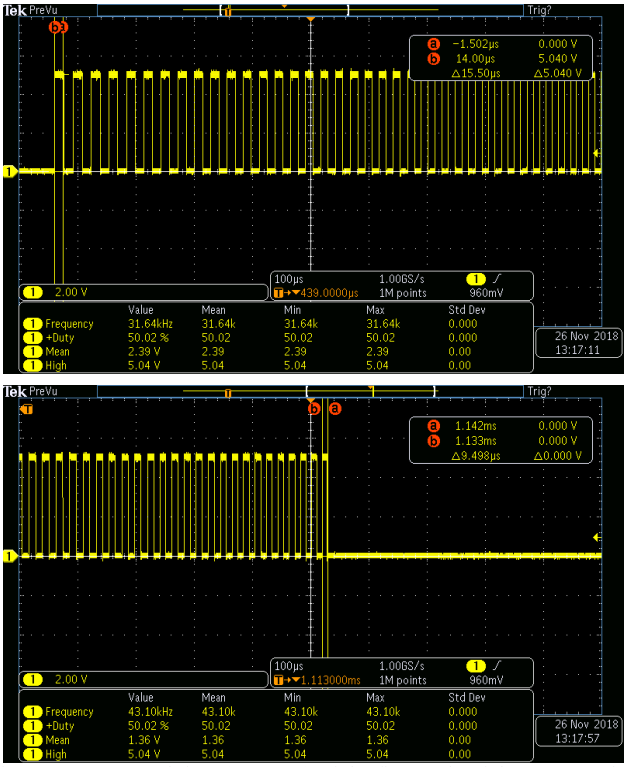

Fig. 3. *Up*, measured time (15.50 µs) of the first cycle of the square pulse. *Down*, Measured time (9.49 µs) of the last cycle of the square pulse. Expected values were 16.6 µs and 10.0 µs, respectively, for frequencies from 30 kHz to 50 kHz (using half cycles).

B. *Algorithm for pulse generation*

Basically, the program turns on and turns off a pin (pin 3 in Fig. 1), at precisely specified times. This part of this program is based on the time spent while the pin is "on" and "off". The timing step was based on all the intermediate frequency divided by 96 (96 spaces in the memory that we used). Each intermediate frequency between 30 kHz and 50 kHz (at steps of 208.33 Hz) was converted to time (half-cycle-time), and then divided by the "time-per-cycle" of a customized loop (to produce a "for" cycle in assembly); this produced a number to loop's steps required to get the original half-cycle-time. Finally, we rounded the found loop steps, so we can change it to a hexadecimal value. We assigned each found value to a different memory space, to be read at each instruction of turn-on/off, before it was sent to the customized "for" with the corresponding value in the memory; this value indicates the time needed to keep the pulse in high or low state ("on" or "off" respectively).

Finally, the synchrony was made using a single instruction at the beginning of the process previously explained, using the pin 4. With this pulse, it is possible to synchronize the measurement either to have the reference to determine the time in which the pulse was initiated, or to keep frozen the signal shown in the oscilloscope and then determine its characteristics.

C. *Switched amplifier*

Power supply voltages depended on the devices used for the circuits. Microcontroller, and therefore the control section, were connected to 5.0 V, while the power section can be set beyond 5.7 V (to effectively turn on the transistor), limited by the maximum voltage tolerated by the transistor. In this case, to avoid too many power supplies, the voltage of the power section was 11.5 V, as the power of the receiving section of ±11.5 V (limited by the operational amplifiers). These power supplies will be separated in future developments.

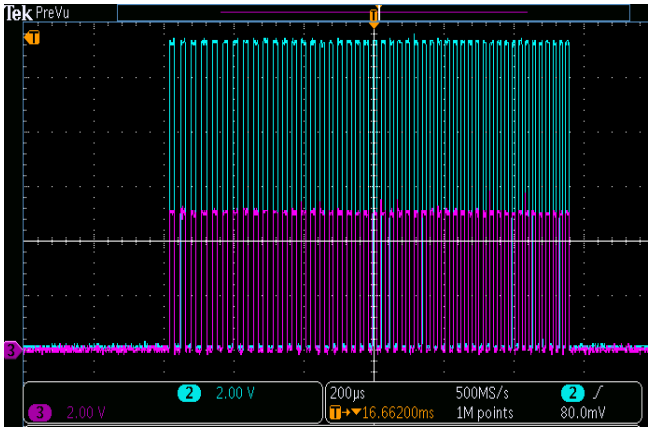

Fig. 4. Oscilloscope image of the control pulse (purple) and the amplified output (blue) on a resistive load of 470 Ω.

In Fig. 4, it can be appreciated the purple signal that is the signal of the microcontroller (the square pulses) and the blue one is that pulse but amplified when using a resistive load of 470 Ω. This means that the device correctly amplified the signal, as we mentioned before, without important heating (maximum 0.7 °C).

In Fig. 5, it is shown the output of the amplifier when the transducer is connected as the load. The amplitude of the time-domain signal varies because of variations in the frequency response of the transducer, which, as mentioned before, has a frequency bandwidth from 35 kHz to 45 kHz. The most planar region of the amplifier output is indeed located between the frequencies in which the transducer has a larger resistance, i.e. just after 35 kHz and before 45 kHz. Near the central frequency (around 40 kHz), the impedance is reduced and the transducer inductive-capacitive components interfere [10], which varies amplitude of the output.

All that mentioned can be checked with other details in the second part of Fig. 5, which shows the spectrogram of the output. In this time-frequency representation, we can notice how the frequency of the generator changed linearly from about 30 kHz to 50 kHz. The amplitude (color) is also dependent on the impedance, giving an important variation at 40 kHz, which is the main operation frequency of the

transducer. Just to clarify, having low amplitude in these graphs around 40 kHz does not mean the transducer is emitting less energy at these frequencies, but only indicates that the impedance is not the same along the graph. The emitted signal will be analyzed later with respect to Fig. 7, showing a larger amplitude at the center (40 kHz).

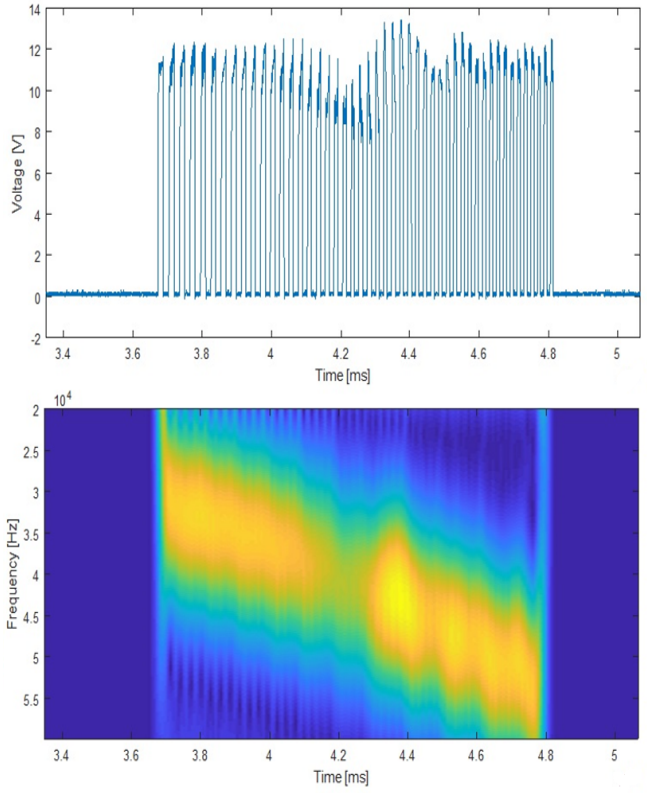

Fig. 5. *Up*, output signal with the transducer as load. *Down*, spectrogram of the output showing a linear sweep in frequency vs time.

Another representation of the previous output is shown in Fig. 6. For this figure, the fast Fourier transform (FFT) was obtained from the data of Fig. 5 to check the full bandwidth of the amplifier output. The obtained spectrum shows that the operation frequency (half of the amplitude) starts at 33 kHz to 51 kHz, very close to the values obtained from the measured on/off cycle time. The center frequency is located at 40 kHz, in which the reduced impedance provoked a down peak at that point. It was expected a planar response at all frequencies, which by looking at Fig. 6, it was not the case. The final ultrasound chirp is shown in Fig. 7, in which it can be noticed that the transducer still response to other frequencies outside the effective range. The larger amplitude corresponds to the central operation frequency of 40 kHz. This is only the characteristic received echo; other analysis of this final signal is beyond the scope of this paper.

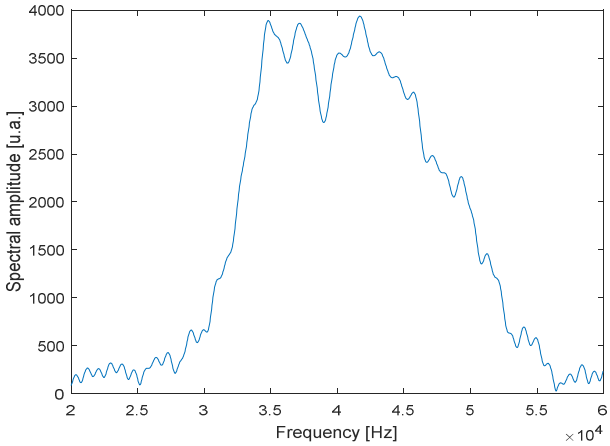

Fig. 6. Spectrum (FFT) of the amplifier output with the transducer as load. The output is enough wide to effectively drive the commercial transducer.

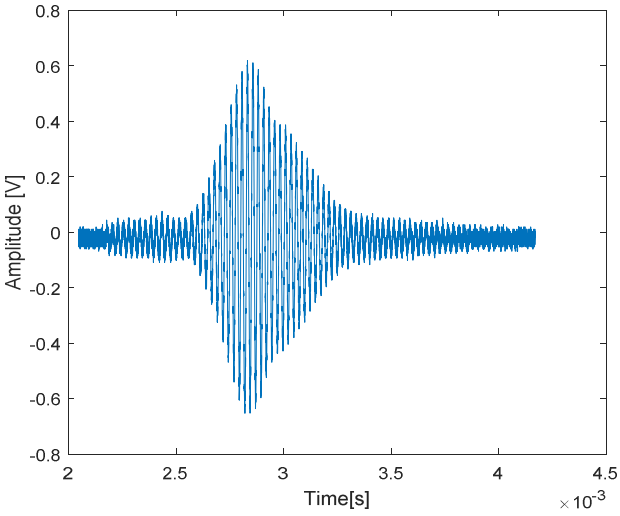

Fig. 7. Received characteristic echo. The initial and final low-power section correspond to the frequencies out of the bandwidth of the transducer.

IV. Conclusion

This paper presented the design of a pulse generator with varying pulse widths that can be related to a sweep of frequency when this is used to drive air coupled ultrasound transducers. When using this sweep of frequency, it is possible to produce a compact multifrequency pulse for material inspection. The use of multiple frequencies instead of only the main one would permit to extract more information from the material to analyze. This work shows the electronic design to be able to propose another possible use of these commercial air coupled transducers. The intended application of this circuit is in obstacle detection/identification for blind people. However, it remains open the possibility of new investigations and applications that potentially could use the circuits proposed in this work, for example, medical applications for a higher frequency transducer for tissue characterizations.

ACKNOWLEDGMENT

Authors would like to thank funding support by CONACyT CB2015-257966, ERAnet-EMHE 200022, and CYTED-DITECROD. RD Casillas would like to thank CONACYT for undergrad thesis scholarship 28144.

REFERENCES

[1] D. Hu, D. Wang, X. Li, F. Nie, and Q. Wang, "Listen to the Image," Apr. 2019.

[2] J. Borenstein and Y. Koren, "Obstacle avoidance with ultrasonic sensors," *IEEE J. Robot. Autom.*, vol. 4, no. 2, pp. 213–218, Apr. 1988.

[3] T. I. Chiu, H. C. Deng, S. Y. Chang, and S. B. Luo, "Implementation of ultrasonic touchless interactive panel using the polymer-based CMUT array," in *Proceedings of IEEE Sensors*, 2009, pp. 625–630.

[4] L. F. Mondragon, A. Vera, L. Leija, J. Gutierrez, J. E. Chong-Quero, and M. I. Gutierrez, "Transceiver system for obstacle detection based on bat echolocation with air-coupled pulse-echo ultrasound," in *2017 14th International Conference on Electrical Engineering, Computing Science and Automatic Control (CCE)*, 2017, pp. 1–5.

[5] D. S. Vidhya, C. J. D. Silva, and C. J. Costa, "Obstacle Detection using Ultrasonic Sensors," *Int. J. Innov. Res. Sci. Technol.*, vol. 2, no. 11, pp. 316–320, 2016.

[6] N. Gageik, P. Benz, and S. Montenegro, "Obstacle Detection and Collision Avoidance for a UAV With Complementary Low-Cost Sensors," *IEEE Access*, vol. 3, pp. 599–609, 2015.

[7] G. Gibbs, H. Jia, and I. Madani, "Obstacle Detection with Ultrasonic Sensors and Signal Analysis Metrics," *Transp. Res. Procedia*, vol. 28, pp. 173–182, Jan. 2017.

[8] T. H. Gan, D. A. Hutchins, D. R. Billson, and D. W. Schindel, "The use of broadband acoustic transducers and pulse-compression techniques for air-coupled ultrasonic imaging," *Ultrasonics*, vol. 39, no. 3, pp. 181–194, 2001.

[9] T. Gómez Alvarez-Arenas and T. E. Gomez Alvarez-Arenas, "Air-Coupled Piezoelectric Transducers with Active Polypropylene Foam Matching Layers," *2011 IEEE Int. Ultrason. Symp. Proc.*, vol. 13, no. 5, pp. 5996–6013, May 2013.

[10] A. Ramos, J. L. San Emeterio, and P. T. Sanz, "Improvement in transient piezoelectric responses of NDE transceivers using selective damping and tuning networks," *IEEE Trans. Ultrason. Ferroelectr. Freq. Control*, vol. 47, no. 4, pp. 826–835, 2000.